

# Quantification of diffuse dust emissions from open air sources on industrial sites

THERESE BADR

Ecole des Mines de Douai  
Department of industrial Energetics  
941 rue Charles Bourseul, 59508 Douai  
FRANCE

JEAN-LUC HARION

Ecole des Mines de Douai  
Department of industrial Energetics  
941 rue Charles Bourseul, 59508 Douai  
FRANCE

*Abstract:* The environmental impacts as well as the economical aspects and regulation constraints related to wind erosion motivate current efforts to model and quantify erosion. The nature of the underlying processes makes quantification of diffuse dust emissions a very demanding exercise that is still subject of active research. Certain aspects were not fully apprehended, others require further development. These include the influence of the wide size distribution of granular materials and the sensitivity of the stockpiles' wind exposure on industrial sites to various parameters, such as the geometry of the pile and its location as well as the wind conditions. The objective of this work is to improve the accuracy of diffuse dust emissions' estimations, by creating precise and detailed databases for existing models. Three-dimensional numerical simulations were developed and validated in order to investigate the sensitivity of the mean flow structure to varying stockpile geometries and wind conditions. A second local approach was also applied, which aims to study flow characteristics and the evolution of the friction velocity at the wall in the presence of nonerodible elements for various configurations and roughness densities. The numerical data can be used in order to improve the current models' accuracy and performance.

*Key-Words:* Aeolian erosion, numerical simulations, emission factors, diffuse emissions

## 1 Introduction

Steel production, power generation and many more industries produce dust emissions that can have a detrimental effect on their nearby environment. With the implementation of proper control methods these effects can be minimized. In order to assess impacts and develop effective solutions, accurate evaluation of diffuse dust emissions is needed. Because direct measurements are expensive and difficult to implement on site, quantification models are used instead. In spite of their regular update, these models still suffer from severe limitations, mostly related to a lack of empirical data of adequate quality and a lack of development of new technologies and equipment. Reverse dispersion modelling is also used to assess on-site emissions and allows the ranking of emission sources. It fails, however, to accurately estimate emitted quantities.

The present work was motivated by a global study concerning the quantification and reduction of diffuse dust emissions on industrial sites with the collaboration of ARCELOR MITTAL (integrated steel works of Dunkerque and Fos-sur-mer), and sponsored by the French Agency for Environment and Energy Management (ADEME). It aims to improve the accuracy of input data for erosion prediction models. It also al-

lows additional insight on the erosion processes and takes into account the impact of relevant parameters such as the wide size particles' distribution. For this purpose, two approaches were attempted using numerical simulations. In the first approach, wind exposure over stockpiles and its variation with the pile configuration and wind conditions was assessed. The second is a local-scale approach that deals with the influence of nonerodible particles on the erosion progression of erodible particles. The use of CFD modelling allows fine and quick monitoring of the spatial changes of airflow over obstacles in response to varying different parameters.

## 2 Wind exposure of storage piles

A common method to quantify diffuse dust emissions is the use of emission factors. The actual model used by ARCELOR MITTAL is an upgraded version of the USEPA emission factor formulation [3] that was developed in collaboration with SECHAUD Environment to take into account important parameters such as meteorological data, storage quantity and location, traffic and transported quantities, and dust size distribution.

Emission factors for open aggregate storage pile sources, according to the USEPA formulation, are function of the piles' wind exposure characterized by a velocity ratio  $u_s/u_r$  [3], where  $u_s$  is the wind speed at  $0.25\text{ cm}$  from the pile surface and  $u_r$  is the reference wind speed at the equivalent full-scale height of  $10\text{ m}$ . The piles are divided into sub-areas of constant  $u_s/u_r$  and each sub-area is considered as a separate source. In the EPA report [3], profiles of  $u_s/u_r$  over two representative pile shapes and for three wind directions were provided along with an approximated surface area within each wind speed regime. These data were derived from wind tunnel studies and show a pronounced influence of the pile geometry and wind direction on the velocity distribution over the piles. However, the stockpiles investigated do not cover the wide variety of pile shapes and dimensions that can be found on industrial sites. This is also true for wind conditions. Since flow patterns are affected by these parameters, more convenient data should be available to accurately estimate emission factors.

Three-dimensional numerical simulations were validated for wind tunnel measurements using the Fluent CFD software. Full verification and validation of the simulations were discussed in an earlier paper [1]. The numerical  $u_s/u_r$  values can be retrieved for each case study to compute emission factors. Apart from its easier application in comparison with the complicated experimental method and the possibility to test various pile configurations more quickly and with least technical equipment, the asset of using this technique is that it provides more detailed data of  $u_s/u_r$  because of the fine spatial resolution when computing velocity distribution over the piles. This should improve the estimation of diffuse particulate emission factors from stockpiles. Figure 1 shows an example of numerical  $u_s/u_r$  contours over a particular stockpile configuration, obtained from numerical simulations.

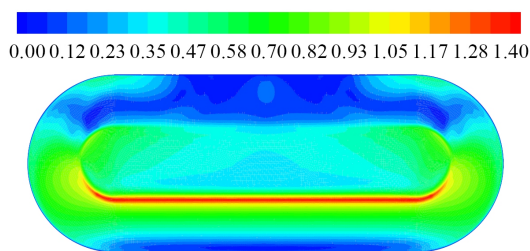


Figure 1: Top view of  $u_s/u_r$  contours over a particular stockpile configuration (airflow is from below)

The numerical simulations were then used to investigate the sensitivity of the mean flow structure to varying stockpile configurations (shape, dimension and location) and wind conditions (magnitude and di-

rection) [2]. These applications allowed additional insight on the understanding of 3D flow processes occurring around stockpiles and their implications on particles' uptake, the assessment of the impact of pile configuration and wind conditions on dust emissions, a more accurate evaluation of emission factors using local wind characteristics near the piles, and the disclosure of the pile configurations that correspond to the lower emission rates for a given wind condition. Additionally, this approach helps determine the best way a definite material quantity should be arranged during storage, according to the dominant wind characteristics of the site, in order to limit wind erosion [2].

### 3 Roughness elements' effect on erosion

Most sedimentary environments subject to aeolian erosion are characterized by a wide size particle distribution. This is also the case for raw materials such as coal or iron ore on steelworks and power plants. With the deflation of erodible particles on the surface under wind action, the concentration of nonerodible aggregates that are bound to the surface by their inertia, increases. These roughness elements act to protect the underlying erodible surface either by covering the surface or by creating lee-side wakes, in which average wind speed is drastically reduced [10]. This is called bed pavement and has direct effects on dust emission rates. Nevertheless, most available models for the estimation of dust emissions apply to particle beds with a homogeneous size distribution [7]. A new approach was proposed to model the temporal evolution in the grain size characteristics of surface aggregates in a wide sized particle bed under aerodynamic erosion conditions [5]. It is based on the close correlation between particles' uptake and turbulent structures in the boundary layer and takes into account the saltation phenomenon, as well as the probability distribution of the adhesive and aerodynamic lift forces acting on a particle. Bed pavement is modelled by an incrementation of the lift force. The model is able to predict the temporal decrease in the emitted mass flux and the grain-size distribution of the eroded aggregates as well. The model results were compared with wind tunnel experimental data using sand with a bimodal size distribution. Erodible particles had a mean diameter of  $\bar{D} = 100\ \mu\text{m}$  and that for nonerodible particles averaged approximately  $\bar{D} = 1.074\ \text{mm}$ . The comparison was performed for different mass fractions and wind velocities, and revealed the influential parameters that require additional investigations; the decay rate needs to be adjusted in the actual version of

the model. This parameter is controlled by the erosion depth (the bed depth at which nearly all the surface is covered with nonerodible particles) which in turn is defined from the lift force increment.

A new approach is proposed that consists in assessing the shear stress evolution on the erodible surface using numerical simulations and compute the aerodynamic lift force evolution accordingly. The erosion depth will be then attained once the friction velocity at the surface reaches the threshold value for the erodible particles considered ( $U_{\tau_S} = U_{\tau_t}$ ). This approach is more in accordance with the physical nature of the process.

### 3.1 Numerical simulations

The shear stress distribution over roughness arrays of varying density, representing the erosion progress on a bed of erodible and nonerodible particles, was studied using the Fluent code. The studied configurations correspond to a bed of granular materials where nonerodible particles (NEP) are represented by randomly distributed spheres, emerging at various levels from the surface. Figure 2 summarizes the principal parameters of the tested configurations. Various roughness densities  $\lambda = nbH/s$ , where  $n$  is the number of roughness elements of width  $b$  and height  $H$  per unit surface area, were simulated. This was achieved by varying the number, diameter  $D$  and the emerging height  $H_s$  (%) of the nonerodible particles. Physically, the smooth case (test 0) corresponds to the beginning of erosion, i.e. where erodible particles entirely cover the surface and nonerodible elements are trapped inside the granular mass. Each particle diameter was treated separately. Eroding particles were not directly simulated, but were appended to the intervening wall surface,  $S$ . The cover rate  $TDC$  represents the surface proportion occupied by the NEP for a given diameter ( $TDC = n\pi D^2/4S$ ).

The computational domain was materialized by a box of dimensions  $3\text{ cm} \times 3\text{ cm} \times 10\text{ cm}$  (Fig. 3). Periodic conditions were applied to the entry and exit. A mass flow rate value corresponding to a mean velocity of  $8\text{ m s}^{-1}$  was used. For this windspeed, the simulated particles ( $D = 1.074$  and  $2\text{ mm}$ ) are considered as nonerodible. The upper and lateral boundaries were defined as symmetry and the lower limit as a smooth wall. These conditions take into account the fact that the simulated bed is not isolated and represents a wider domain. The influence of the particles' distribution was studied to ensure that the studied domain sample is fairly representative. Second-order discretisation schemes were used for the numerical solution (pressure terms and all other variables) to increase the accuracy and reduce numeri-

N° test	TDC (%)	D (mm)	H <sub>s</sub> (%)	n	H (mm)	λ
0	0	0	0	0	0	0
1	5	2	5	14	0.10	0.00135
2	5	2	10	14	0.20	0.00375
3	5	2	15	14	0.30	0.00676
4	5	2	20	14	0.40	0.01023
5	5	2	30	14	0.60	0.01833
6	5	2	40	14	0.80	0.02684
7	5	1.074	10	49	0.11	0.00331
8	5	1.074	20	49	0.21	0.00906
9	5	1.074	30	49	0.32	0.01605
10	5	1.074	40	49	0.43	0.02376
11	10	2	10	28	0.20	0.00748
12	10	2	20	28	0.40	0.02046
13	10	2	30	28	0.60	0.03626
14	10	2	40	28	0.80	0.05368
15	10	1.074	10	99	0.11	0.00669
16	10	1.074	20	99	0.21	0.01830
17	10	1.074	30	99	0.32	0.03243
18	10	1.074	40	99	0.43	0.04802
19	15	2	10	42	0.20	0.01122
20	15	2	40	42	0.80	0.08053
21	15	1.074	10	149	0.11	0.01007
22	15	1.074	40	149	0.43	0.07227
23	20	2	10	57	0.20	0.01522
24	20	2	20	57	0.40	0.10929
25	20	2	30	57	0.60	0.04165
26	20	2	40	57	0.80	0.07382

Figure 2: Characteristic parameters of the simulated configurations

cal diffusion. The SimpleC algorithm was used for pressure-velocity coupling. All the residuals were set to  $10^{-5}$ . It was considered that convergence will not be attained unless velocity and turbulence profiles become fully developed at the entry. Turbulence closure was achieved through application of the two-equation  $k - \omega - SST$  Transitional Flow model developed by Menter [8]. This turbulence model takes into account the low-Reynolds-number effects. Its eddy-viscosity formulation also accounts for the principal turbulent shear stress, making it appropriate for the prediction of adverse pressure gradient flows [8]. The turbulence closure model as well as the grid resolution were checked to ascertain the robustness of the model and the accuracy of its results.

The simulations results were compared and appeared to be in good agreement with experimental data from various authors [4, 9, 6]. The numerical  $R_t$  values, the ratio of the shear stress of the intervening surface area to the total stress, were within the experimental error estimated to  $\pm 20\%$  approximately [4].

### 3.2 Results and discussion

The evolution of friction velocity on the intervening surface, representing erodible particles, was analyzed with respect to the cover rate, the emerging height and the density  $\lambda$  of nonerodible particles. The effect of each of these parameters was studied. Results show that an increase in both, the cover rate and the height of roughness elements will lead to a total suppression of erosion. These two parameters control the variation

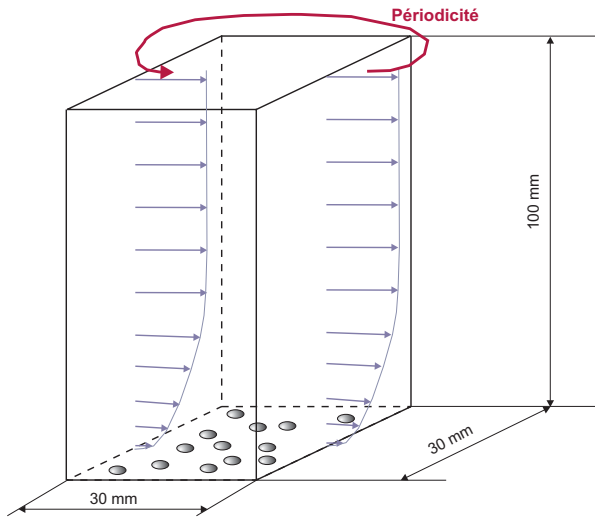


Figure 3: Representation of the numerical domain

of  $\lambda$ , but their influence on this variation, as well as on the friction velocity distribution and evolution is different. Indeed, flow disturbances near the surface are controlled by pressure gradients induced by the presence of nonerodible particles. The simulations show that for low  $H$  configurations, the flow circumvents the particle without separating from the surface which limits the zone of low friction velocity in the lee. With roughness height increase, pressure gradients become sufficiently important to induce a flow separation on the sides and the development of a larger wake region downstream. The extent of the wake surface is hence function of the roughness height (Fig. 4) and constitutes a shelter area for the underlying fine-grained particles. Figure 4 also illustrates the cover rate effect on the distribution of  $U_{\tau_s}$ . No wake interactions are observed for the low  $H$  configurations even with the particle's number increase and a large part of the surface remains subject to erosion. With the increase in both the  $TDC$  and  $H$ , wakes expand and start to interact with the neighbouring particles leading to a drop in friction velocity on most of the intervening surface area.

The use of numerical simulations to supplement experimental methods in assessing the shear stress evolution at the erodible surface should allow additional insights and understanding of certain aspects of the problem until now not fully apprehended because of logistical and instrumentation limitations. Numerical techniques have the advantage to be cheaper and allow fast and controlled variation of different parameters, which is difficult to realize in wind tunnel experiments and nearly impossible on site for such applications. Additionally, accurate characterization of the shear stress evolution with the erosion progression is of great importance since this parameter affects the

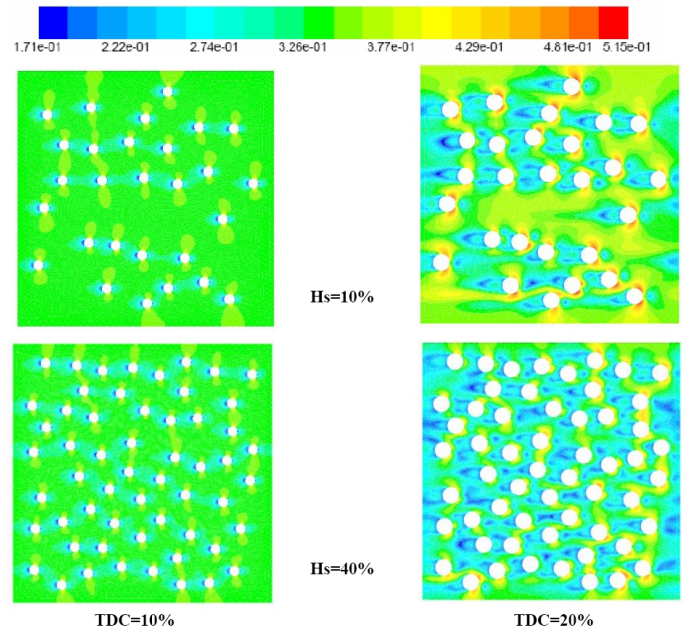


Figure 4: Top view of friction velocity contours at the intervening surface  $U_{\tau_s}$  for different cover rates  $TDC$  and emerging heights  $H_s$  of nonerodible particles with  $D = 2\text{ mm}$  (airflow is from the left).

wind capacity to entrain particles and hence controls erosion. The numerical data will be integrated in the aeolian erosion model for multiple-sized particle beds introduced earlier to improve its performance.

## 4 Conclusion

Diffuse dust emissions constitute a major concern for many industrial sectors. Despite the great number of studies conducted to quantify and limit emissions, this issue remains the subject of large investment. The ability to accurately predict wind erosion is essential for, among other things, reducing air pollution. This paper constitutes a computational effort for a better quantification and prediction of diffuse dust emissions. It introduces new approaches to estimate emission rates from aggregate storage pile sources and for multiple-sized particle beds more accurately using data from CFD modelling.

These improvements will be integrated in a new software for the quantification of dust emissions from open sources based on an upgraded version of the USEPA emission factor formulations. This application will be developed in a protected Internet technology that is easy to use and update.

**Acknowledgements:** The research was supported by ADEME (the French Agency for Environment

and Energy Management) and ARCELOR MITTAL Dunkerque/Fos-sur-Mer (steelworks in France).

*References:*

- [1] T. Badr and J.-L. Harion, Numerical modelling of flow over stockpiles: implications on dust emissions, *Atm. Env.* 39, 2005, pp. 5576–5584.
- [2] T. Badr and J.-L. Harion, Effect of aggregate storage pile geometries on dust emissions, *Atm. Env.* 41, 2007, pp. 360–368.
- [3] EPA, Midwest research institute, Kansas City, AP-42 section 11.2 – wind erosion, MRI No. 8985-K *Update of fugitive dust emissions factors in AP-42*, 1988.
- [4] D.-A. Gillette and P.-H. Stockton, The effect of nonerodible particles on the wind erosion of erodible surfaces, *J. Geoph. Res.* 94, 1989, pp. 12885–12893.
- [5] I. Descamps, *Érosion éolienne d'un lit de particules à large spectre granulométrique*, PhD thesis École des Mines de Douai, 2004.
- [6] L. Lyles and R.-L. Schrandt and N.-F. Schmeidler, How aerodynamic roughness elements control sand movement, *Trans. ASAE* 17, 1974, pp. 134–139.
- [7] B. Marticorena and G. Bergametti, Modeling the atmospheric dust cycle: 1. Design of a soil-derived dust emission scheme, *J. Geophys. Res.*, 100, 1995, pp. 16415–16430.
- [8] F.-R. Menter, Two-Equation Eddy-Viscosity Turbulence Models for Engineering Applications, *AIAA J.*, 32, 1994, pp. 1598–1605.
- [9] H.-B. Musick and D.-A. Gillette, Field evaluation of relationships between a vegetated structural parameter and sheltering against wind erosion, *Land. Degrad. Rehabil.*, 2, 1990, pp. 87–94.
- [10] C. Neuman, Particle transport and adjustments of the boundary layer over rough surfaces with an unrestricted, upwind supply of sediment, *Geom.*, 25, 1998, pp. 1–17.